

**LA-7778-MS**

Informal Report

C.3

**REPRODUCTION  
COPY**

CIC-14 REPORT COLLECTION

**MHD Deceleration of Fusion Reaction Products**

University of California



**LOS ALAMOS SCIENTIFIC LABORATORY**

Post Office Box 1663 Los Alamos, New Mexico 87545

**An Affirmative Action/Equal Opportunity Employer**

This report was prepared as an account of work sponsored by the United States Government. Neither the United States nor the United States Department of Energy, nor any of their employees, nor any of their contractors, subcontractors, or their employees, makes any warranty, express or implied, or assumes any legal liability or responsibility for the accuracy, completeness, or usefulness of any information, apparatus, product, or process disclosed, or represents that its use would not infringe privately owned rights.

LA-7778-MS  
Informal Report  
UC-21  
Issued: April 1979

## MHD Deceleration of Fusion Reaction Products

S. Chow\*  
I. O. Bohachevsky



\*Graduate Research Assistant. School of Engineering, Georgia Institute of Technology,  
Atlanta, GA 30332.



# MHD DECELERATION OF FUSION REACTION PRODUCTS

by

S. Chow and I. O. Bohachevsky

## ABSTRACT

The feasibility of magnetohydrodynamic (MHD) deceleration of fuel pellet debris ions exiting from an inertial confinement fusion (ICF) reactor cavity is investigated using one-dimensional flow equations. For engineering reasons, induction-type devices are emphasized; their performance characteristics are similar to those of electrode-type decelerators. Results of the analysis presented in this report indicate that MHD decelerators can be designed within conventional magnet technology to not only decelerate the high-energy fusion pellet debris ions but also to produce some net electric power in the process.

## I. INTRODUCTION

The magnetically protected laser fusion reactor cavity design, shown in Fig. 1, has been proposed<sup>1</sup> and is being developed at the Los Alamos Scientific Laboratory (LASL). In this concept, the reactor cavity wall is protected from charged particles generated in the fuel pellet microexplosion by a magnetic field which diverts the ions into conical energy sinks. Although these sinks are inexpensive and easily replaced, calculations<sup>2</sup> indicate that their high sputtering erosion rate may result in an economically unacceptable replacement frequency.

To overcome this problem, we have proposed to replace the energy sinks with MHD decelerators,<sup>3</sup> shown schematically in Fig. 2. Preliminary calculations indicate<sup>3</sup> that the device may generate

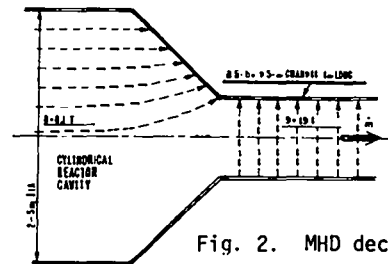


Fig. 2. MHD decelerator principle.

enough electric power to offset joule losses in the electromagnet windings so that the MHD decelerator could be self-sustaining.

In this report we will describe a more extensive, albeit still only preliminary, one-dimensional analysis of the applicability of MHD generators to inertial confinement fusion reactor designs. We have imposed two requirements on these devices to establish the feasibility of MHD deceleration of fusion reaction products: (a) the cavity exhaust velocity should be reduced to a value at which the products, with perhaps the aid of diffusers, can be used in a conventional heat exchanger, and (b) the deceleration process should generate a sufficient quantity of electricity to power the required magnets.

The presentation is organized as follows. In Sec. II we discuss MHD deceleration in general, point out the two ways of extracting the energy from the process: either with electrodes or with

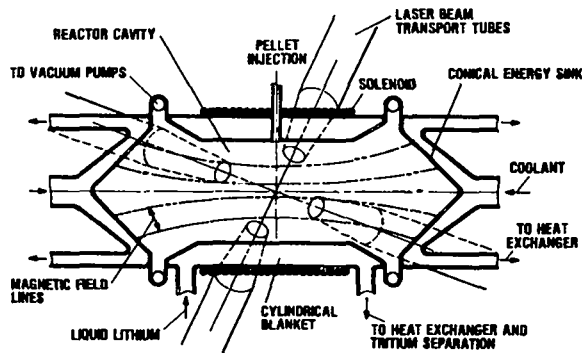


Fig. 1. Magnetically protected laser fusion reactor cavity.

induction coils and discuss the advantages of the latter for our current application. In Sec. III we set up the governing equations and discuss their analysis, and in Sec. IV we present the results showing parametric dependencies of the operating characteristics. The implications of these results bearing on the intended application are discussed in the closing section.

II. MHD DECELERATION

A. Conventional (with Electrodes)

Magnetohydrodynamic (MHD) deceleration is the application of the Lorentz force to a moving conducting plasma. The concept which has received most attention is the MHD generator with electrodes shown schematically in Fig. 3. A conductor passing through a magnetic field, induces an electric field so that if electrodes and electric load are added, a current proportional to the current density will flow through the load.

Various geometries and electrodes may be used depending on specific design objectives. Our interest is in generators which decelerate the flow and are relatively simple to model. Therefore, we will ignore the Hall current and will consider an MHD generator with rectangular cross-sectional area and continuous electrodes.

The major limitation of MHD generators is wall erosion resulting in the short lifetime of

the electrodes. For example, copper anodes with platinum caps and copper cathodes with tungsten-copper caps developed by AVCO for the coal-fired MHD program have survived only a 250-h test.<sup>4</sup> However, economical power plant operation may require electrode lifetimes of 10000 h or more.

In MHD generators exposed to laser fusion products immediately after their exit from the reactor cavity, electrode erosion is likely to be more severe than in coal-fired generators, because the fusion-generated plasma exits the reactor cavity at a much higher velocity ( $10^4$ m/s as opposed to  $10^3$ m/s for combustion-generated plasma), and contains a large amount of metallic ions. In addition, chemical reactions between the fusion products and electrodes may also be detrimental. Therefore, it may be extremely difficult, if not impossible, to develop long-lived electrodes for the conditions anticipated in fusion-reactor-driven MHD generators.

B. Induction-Type MHD Decelerators

To avoid the electrode erosion problem, an induction-type MHD generator may be used. In this concept, the electrodes are replaced by insulator walls and induction coils are placed on the faces of the magnet, as shown schematically in Fig. 4. A slug of plasma passing through the channel induces a current that generates a magnetic field.

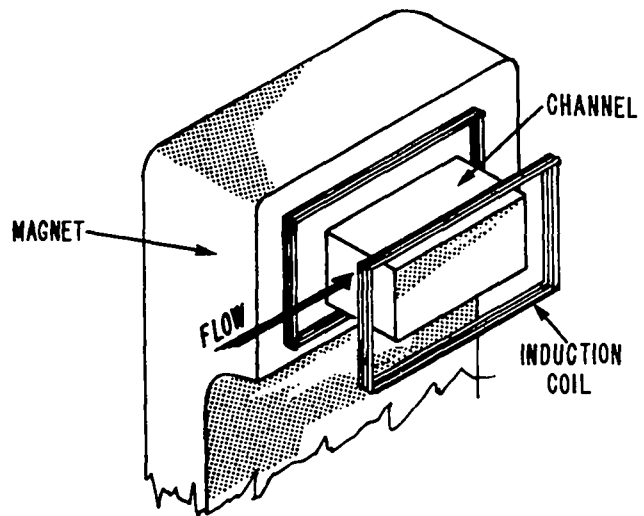
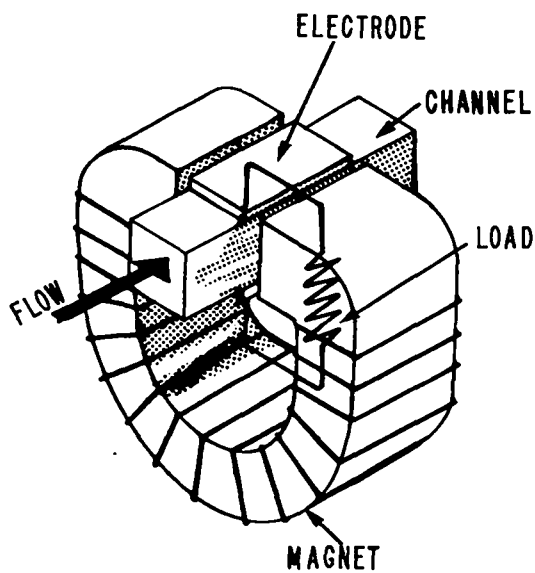


Fig. 3. MHD generator with electrodes.

Fig. 4. Induction-type MHD generator.

The resulting change in the magnetic flux produces an electromotive force in the output coils.

The induction-type generator was first proposed by Colgate and Aamodt<sup>5</sup> for energy extraction from plasmas produced in fission reactors. More recently, Velikhov et al.<sup>6</sup> proposed an induction-type generator in which laser fusion products accelerate a solid or liquid metal piston, and the kinetic energy is extracted as the piston moves through the magnetic field. The use of laser fusion plasma itself for induction of an electromotive force in coils was first studied by Roberts<sup>7,8</sup> and by Wood et al.<sup>9-11</sup>

The power density of an induction-type generator is a function of the magnetic Reynolds number,  $R_m$ , which is proportional to the product of electric conductivity and velocity. Most combustion-produced plasmas have conductivities and velocities such that  $R_m \ll 1$ . Because MHD programs in this country and in the Soviet Union have focused on coal-fueled combustion as the energy source, little effort has been devoted to the development of induction-type generators. Consequently, our understanding of these devices is not as advanced as that of MHD generators with electrodes.

However, induction-type generators should be considered for laser fusion reactors because, with fusion drivers, the magnetic Reynolds number may be on the order of unity. In addition, in this application only enough power must be generated to make the MHD system self-sustaining; efficiency, therefore, is of secondary importance.

### III. ANALYSIS OF MHD DECELERATORS

#### A. Basic MHD Equations

Assuming steady-state flow and neglecting viscous and heat conduction terms, the continuity, momentum, and energy equations are<sup>12</sup>:

$$\nabla \cdot (\rho \bar{v}) = 0, \quad (1)$$

$$\rho(\bar{v} \cdot \nabla)\bar{v} = -\nabla P + \bar{j} \times \bar{B}, \quad (2)$$

and

$$\rho \bar{v} \cdot \nabla e = -P \nabla \cdot \bar{v} + \frac{j^2}{\sigma}, \quad (3)$$

where  $\rho$  is the density,  $\bar{v}$  the velocity,  $P$  the pressure,  $\bar{j}$  the current density,  $\bar{B}$  the magnetic

field,  $e$  the internal energy, and  $\sigma$  the plasma electric conductivity.

For the purposes of this study, a quasi-one-dimensional analysis will be employed in which the magnetic field is postulated to be perpendicular to the flow velocity,  $u$ . With this hypothesis, Eqs. (1)-(3) reduce to

$$\rho u A = \dot{m} = \rho_0 u_0 A_0, \quad (4)$$

$$\rho u \frac{du}{dx} = -\frac{dP}{dx} - jB, \quad (5)$$

and

$$\rho u \frac{de}{dx} = -P \frac{du}{dx} + \frac{j^2}{\sigma}, \quad (6)$$

where  $\dot{m}$  is the mass flow rate and the subscript 0 refers to conditions at the channel inlet.

Assuming that the medium is a perfect gas:

$$e = c_v T = \frac{1}{\gamma - 1} \frac{P}{\rho}, \quad (7)$$

where  $c_v$  is the specific heat at constant volume,  $\gamma$  the ratio of specific heats, and  $T$  the temperature. Substituting Eq. (7) into Eq. (6) yields

$$\frac{1}{\gamma - 1} \left( u \frac{dP}{dx} - \frac{Pu}{\rho} \frac{d\rho}{dx} \right) = -P \frac{du}{dx} + \frac{j^2}{\sigma}. \quad (8)$$

Logarithmic differentiation of Eq. (4) results in

$$\frac{1}{\rho} \frac{d\rho}{dx} + \frac{1}{u} \frac{du}{dx} + \frac{1}{A} \frac{dA}{dx} = 0. \quad (9)$$

Substituting  $(dP/dx)$  and  $(1/\rho)(d\rho/dx)$  from Eqs. (5) and (9), respectively, into Eq. (8) yields

$$\frac{du}{dx} = \frac{(\gamma - 1) \frac{j^2}{\sigma} + u j B - \frac{Pu}{A} \frac{dA}{dx}}{\gamma P - \rho u^2}. \quad (10)$$

Using the definitions of the speed of sound,  $c$ ,

$$c = \sqrt{\gamma \frac{P}{\rho}}, \quad (11)$$

and of the Mach number,  $M$ ,

$$M = \frac{|u|}{c}, \quad (12)$$

Eq. (10) can be written:

$$\frac{du}{dx} = \frac{1}{M^2 - 1} \left[ \frac{1}{\gamma} \frac{u}{A} \frac{dA}{dx} - \frac{(\gamma - 1)}{\rho c^2} \frac{j^2}{\sigma} - \frac{u}{\rho c^2} jB \right]. \quad (13)$$

Equations (13), (5), and (9) determine  $u$ ,  $P$ , and  $\rho$ , once  $j$ ,  $B$ , and the geometry are specified.

Conditions for a decelerating flow,  $(du/dx) < 0$ , can be deduced from Eq. (13); they are listed in Table I.

It is interesting to compare cases with and without the electromagnetic terms. As can be seen from Table I, supersonic flow can be decelerated in a diverging channel, provided  $(dA/dx) < \Phi$ , whereas, in the absence of electromagnetic forces, supersonic flow can be decelerated only in a converging channel. This is also true for a constant

area channel,  $(dA/dx)=0$ , in which supersonic flow is decelerated when electromagnetic forces are present, but remains at constant velocity when electromagnetic forces are absent. The constant-area case is of interest because the design is extremely simple. For decelerating subsonic flow,  $(dA/dx) > \Phi$  when electromagnetic forces are present, but  $(dA/dx) > 0$  suffices when electromagnetic forces are absent. Therefore, the addition of electromagnetic forces results in a larger channel.

#### B. Equations for MHD Decelerators with Electrodes

To determine the velocity distribution from Eq. (13), expressions for  $j$  and  $B$  are required. For an MHD channel with electrodes, the induced magnetic field can be neglected so that the magnetic field equals the applied magnetic field,  $B_0$ , and  $j$  is determined from Ohm's Law, i.e.,

$$B = B_0, \quad (14)$$

and

$$j = \sigma(uB - E), \quad (15)$$

where  $E$  is the electric field. Introducing the load factor,  $K$ , defined by

$$K = \frac{E}{uB} \quad (16)$$

( $0 < K < 1$  for electric power generation), Eq. (15) becomes

$$j = \sigma uB(1 - K). \quad (17)$$

The power density is given by

$$q''' = Ej = \sigma u^2 B^2 K(1 - K). \quad (18)$$

Clearly, the power density is maximum when  $K=1/2$ , which corresponds to the case when load resistance is equal to the generator internal resistance.

TABLE I

REGIONS OF POSITIVE AND NEGATIVE VELOCITY GRADIENT

$$\Phi = \frac{A\gamma}{\rho c^2} \left[ (\gamma - 1) \frac{j^2}{\sigma} + u j B \right]$$

Without Electromagnetic Effects, $\Phi = 0$			With Electromagnetic Effects, $\Phi = 0$		
$dA/dx$	$M$	$du/dx$	$dA/dx$	$M$	$du/dx$
0	$< 1$	0	0	$< 1$	+
0	$> 1$	0	0	$> 1$	-
+	$< 1$	-	$> \Phi$	$< 1$	-
+	$> 1$	+	$> \Phi$	$> 1$	+
-	$< 1$	+	$\Phi$	$< 1$	0
-	$> 1$	-	$\Phi$	$> 1$	0
			$< \Phi$	$< 1$	+
			$< \Phi$	$> 1$	-

The power generated as a function of axial position,  $x$ , is

$$\dot{q} = \int_0^x K(1-K) u^2 B^2 \sigma A dx', \quad (19)$$

and therefore, the total power generated in a channel of length  $L$  is

$$\dot{Q}_{eL} = \dot{q}(L). \quad (20)$$

The voltage developed between the electrodes is given by

$$V = KuBb, \quad (21)$$

where  $b$  is the channel height in the direction of the electric field.

#### C. Equations for Induction-Type MHD Generator

The analysis for the induction-type generator follows that of Ref. 13. An important parameter in generators of this type is the magnetic Reynolds number, defined by

$$R_m = \frac{\sigma \mu_0 u a}{\pi}, \quad (22)$$

where  $\mu_0$  is the permeability of free space,

$$\mu_0 = 4\pi \times 10^{-7} \frac{V-s}{A-m},$$

and  $a$  is the channel width in the direction of the magnetic field.

The induced current density of

$$j = \frac{1}{4} \sigma u B_0 \quad (23)$$

produces an induced magnetic field given by

$$B_i = R_m B_0. \quad (24)$$

Therefore, the magnetic field in the channel is composed of both the applied and the induced magnetic fields

$$B = B_0 + B_i. \quad (25)$$

Equations (22) through (25) may be used in Eq. (13) to determine the velocity distribution.

The available power as a function of position is given by

$$\dot{q} = \int_0^x \frac{1}{4} \sigma u^2 B_0^2 R_m A dx'. \quad (26)$$

Note the similarity between Eqs. (19) and (26). When  $K=1/2$ , corresponding to the maximum power density, Eq. (26) differs from Eq. (19) in the integrand by the factor of the magnetic Reynolds number. In coal-fired MHD generators,  $R_m \ll 1$  and the powers produced by induction-type generators are too low to be of practical interest. However, this may not be the case in laser fusion plasmas.

The power given by Eq. (26) is maximum at  $x=L$ , i.e.,

$$\dot{Q}_{MAX} = \dot{q}(L). \quad (27)$$

The self-generated magnetic field induces voltage in the coil according to Faraday's Law of Induction; therefore, the voltage in the coil as a function of position is

$$V = \int_0^x \frac{n_{IC}}{L} b u B_i dx', \quad (28)$$

where  $n_{IC}$  is the number of turns in the coil and  $b$  the channel height. The total voltage across the coil is

$$V_{IC} = V(L). \quad (29)$$



The current flowing through the coil,  $I_{IC}$ , may not exceed  $I_{MAX} = I_p/n_{IC}$ , where  $I_p$  is the plasma current, or a stronger opposing field would be produced. Therefore, the actual electrical power generated is

$$\dot{Q}_{eL} = V_{IC} I_{IC} < \dot{Q}_{MAX}, \quad (30)$$

where  $I_{IC}$  is chosen in such a way that the inequality is satisfied.

However, there is also a loss term due to ohmic heating of the induction coil given by

$$\dot{Q}_{\Omega IC} = I_{IC}^2 R_{IC}, \quad (31)$$

where the resistance of the induction coil is

$$R_{IC} = \frac{\rho_{IC} L_{IC}}{A_{IC}}. \quad (32)$$

Here  $\rho_{IC}$  is the resistivity of the coil,  $L_{IC}$  is the length of the coil, and  $A_{IC}$  is the cross-sectional area of the coil wire.

Therefore, the net power from the induction coil is

$$\dot{Q}_{netIC} = \dot{Q}_{eL} - \dot{Q}_{\Omega IC}. \quad (33)$$

#### D. Magnet Specification and Net Power Output

The design analysis of the magnet is the same for both MHD concepts. A U-shaped iron magnet core with an air gap generates the magnetic field and steady-state operation of the magnet is assumed in this analysis. Pulsed or superconducting magnets may reduce or completely eliminate ohmic heating losses in the magnet coils but these systems may be too expensive. Therefore, we will examine only the possibility of utilizing a conventional magnet.

To generate a magnetic field,  $B_0$ , with an air gap,  $d_{gap}$ , requires the following number of ampere turns

$$At = \frac{B_0 d_{gap}}{\mu_0}, \quad (34)$$

which implies that the current through the magnet coil is

$$I_{MC} = \frac{At}{n_{MC}}, \quad (35)$$

where  $n_{MC}$  is the number of turns in the winding. The magnet arc length is

$$S_M = d_{MC} m_{MC}, \quad (36)$$

where  $d_{MC}$  is the diameter of the magnet coil wire and  $m_{MC}$  is the number of turns per layer of coil.

Finally, the ohmic heating loss is

$$\dot{Q}_{\Omega MC} = I_{MC}^2 R_{MC}, \quad (37)$$

where the resistance of the magnet coil is given by

$$R_{MC} = \frac{\rho_{MC} L_{MC}}{A_{MC}}, \quad (38)$$

where  $\rho_{MC}$  is the resistivity,  $L_{MC}$  is the length of coil wire, and  $A_{MC}$  is its cross-sectional area.

In our MHD decelerator model, the magnet operates in steady state, but power is produced in pulses because fusion reactions occur in discrete pulses. The duration of a pulse is

$$t_{pulse} = \int_0^L \frac{dx}{u}. \quad (39)$$

Given the repetition rate,  $n_{pulse}$ , the net power from a MHD system with electrodes is

$$\dot{Q}_{net} = \dot{Q}_{eL} n_{pulse} t_{pulse} - \dot{Q}_{\Omega MC}, \quad (40)$$

where  $\dot{Q}_{eL}$  is given by Eq. (20) and  $\dot{Q}_{\Omega MC}$  by Eq. (37).

For the inductive MHD system, the net system power is

$$\dot{Q}_{net} = \dot{Q}_{netIC} n_{pulse} t_{pulse} - \dot{Q}_{\Omega MC}, \quad (41)$$

where  $\dot{Q}_{netIC}$  is given by Eq. (33).

#### IV. RESULTS

##### A. General

The values of many parameters introduced in our analysis are not known accurately; they will be determined by commercial fuel pellet designs and reactor cavity phenomena. The values we used to calculate the results presented in this report are listed in Table II. The estimated mass flow rate,  $\dot{m}$ , is based on an assumed pellet material throughput of  $10^{-2}$  kg/s (through two MHD channels) and on an ion pulse length of  $\sim 100 \mu s$  obtained from numerical simulations of cavity phenomena.<sup>14</sup> In addition, we postulated that the magnet and the induction coils will be made of copper with resistivity of  $1.75 \times 10^{-8} \Omega \cdot m$  at room temperature.

Three types of MHD decelerators were investigated, differing in channel geometry and flow regime: (1) constant area supersonic, (2) diverging supersonic, and (3) diverging subsonic. A converging supersonic channel may also be used to decelerate the flow (Table I), however, it was not

TABLE II

##### PARAMETERS KEPT CONSTANT IN THE STUDY

Instantaneous mass flow rate, $\dot{m} = 5$ kg/s
MHD channel inlet velocity, $U_0 = 10^4$ m/s
MHD channel inlet pressure, $P_0 = 10^5$ N/m <sup>2</sup> (1 atm)
Ratio of specific heats, $\gamma = 1.2$
Pulse repetition rate, $n_{PULSE} = 10$ Hz

considered in detail because preliminary estimates showed that, because of its small volume, its power output will be significantly lower than that of the other geometries.

##### B. Induction-Type MHD Decelerators

###### 1. Constant area supersonic channel

To attain supersonic flow at the conditions stated in Table II, the inlet area must be less than  $0.42 \text{ m}^2$ . We decided to avoid the complications associated with the modeling of sonic transition and therefore specified a magnetic field strength,  $B_0$ , which would ensure that nearly sonic conditions obtain at the channel exit.

Another important parameter in the design of MHD generators is the plasma conductivity,  $\sigma$ . Unfortunately, the composition and the degree of ionization of the fusion products at the channel inlet is not known; it may also vary significantly along the channel length. In this study we postulated that  $\sigma$  remains constant and to determine the effect of its variation we carried out the calculations for different values of  $\sigma$  in the range  $100 \leq \sigma \leq 1000$  mho/m. We chose this range because 1000 mho/m is known to be a very high conductivity plasma and, as will be shown later, 100 mho/m is the lowest conductivity at which an induction generator can produce self-sustaining power for the conditions stated in Table II.

The analysis of the MHD system consisted of two parts. The first part encompassed the analysis of the channel and the second part the design of the induction coils and magnet.

Table III is the list of the parameters for 0.5m by 0.5m by 1m and 0.35m by 0.35m by 1m channels for  $\sigma=1000, 500, \text{ and } 100$  mho/m. Clearly the channel with the smaller cross-sectional area is superior. Reducing the inlet area increases the inlet Mach number,  $M_0$ , from 1.29 to 1.84, and produces a larger drop in the Mach number, which results in a lower exit velocity and a higher power output. The exit Mach number,  $M_f$ , is kept between 1.0 and 1.05 by adjusting  $B_0$ . (It is difficult to obtain the same  $M_f$  without numerous iterations and therefore exit Mach numbers are not exactly equal).

The magnetic field required to decelerate the flow to near-sonic conditions is presented in Fig. 5 as a function of  $\sigma$  for the two inlet

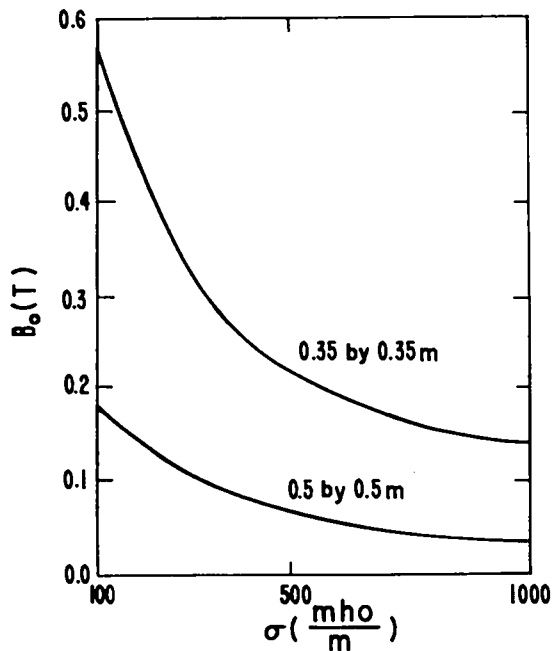


Fig. 5. Magnetic field required to decelerate plasma to near sonic conditions in a constant area duct.

areas. The plots show that the smaller cross section requires larger fields and that the required field strength increases sharply with decreasing  $\sigma$ .

However, note that the field in each case is weak by present technology standard, i.e.,  $B_0 < 1$  T, and that the power output is small.

$\dot{Q}_{IDEAL}$  in Table III is equal to the product of  $\dot{Q}_{MAX}$  defined by Eq. (27),  $n_{PULSE}$ , and  $t_{PULSE}$ . It is the power per pulse developed in the channel and is the maximum power available from the MHD system if losses in the induction coils and magnet are absent, and if the induction

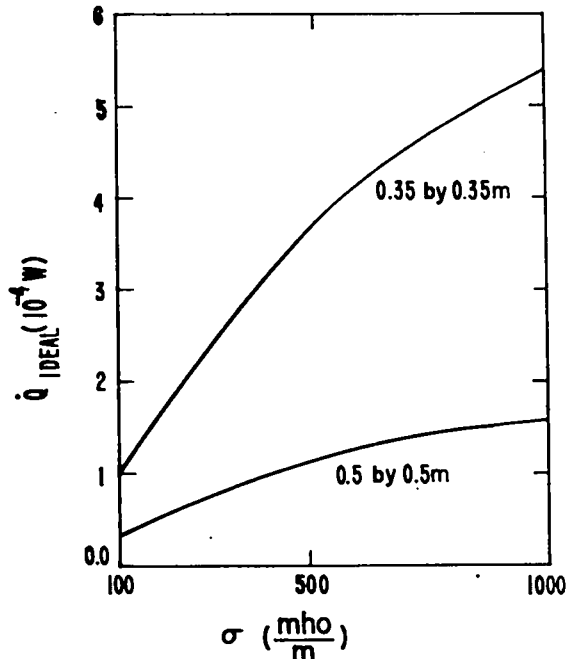


Fig. 6. Ideal power versus conductivity for a constant area supersonic channel.

coil current,  $I_{IC}$  is chosen to be  $I_{MAX}$  associated with  $\dot{Q}_{MAX}$  in Eq. (30). Therefore, it also is the ideal power output of the system. Figure 6 shows that  $\dot{Q}_{IDEAL}$  increases with  $\sigma$  and is higher for the smaller channel.

The parameters in Table III not discussed above are insensitive to the conductivity. The velocities at the exit,  $U_f$ , are roughly 8000 and 5800 m/s for the large and small channels, respectively. A plot of velocity as a function of axial position for the 0.35- by 0.35-m channel at  $\sigma = 1000$  mho/m, shown in Fig. 7, demonstrates an almost linear dependence. The exit pressure,  $P_f$ , listed in Table III increases from the inlet value of  $10^5$  N/m<sup>2</sup> and the increase depends only on the cross-section area to a close approximation.

Because the performance of the 0.35- by 0.35-m channel is superior to that of the 0.5- by 0.5-m one in both flow deceleration and power production, the latter will not be considered further.

The second part of the MHD decelerator analysis was concerned with the design of the induction coils and magnet. A variety of designs can be used; here we will present only representative

TABLE III  
CONSTANT AREA SUPERSONIC DECELERATORS

	0.5- by 0.5- by 1-m channel			0.35- by 0.35- by 1-m channel		
	0.5	0.5	0.5	0.35	0.35	0.35
$a$ (m)	0.5	0.5	0.5	0.35	0.35	0.35
$b_0$ (m)	0.5	0.5	0.5	0.35	0.35	0.35
$L$ (m)	1	1	1	1	1	1
$B_0$ (T)	0.0376	0.0645	0.178	0.134	0.219	0.576
$\sigma$ (mho/m)	1000	500	100	1000	500	100
$M_0$	1.291	1.291	1.291	1.844	1.844	1.844
$M_f$	1.016	1.010	1.048	1.007	1.001	1.006
$U_f$ (m/s)	8045	8006	8284	5784	5767	5812
$P_f$ (N/m <sup>2</sup> )	$1.30 \times 10^5$	$1.30 \times 10^5$	$1.25 \times 10^5$	$1.94 \times 10^5$	$1.81 \times 10^5$	$1.95 \times 10^5$
$t_{PULSE}$ (s)	$1.08 \times 10^{-4}$	$1.08 \times 10^{-4}$	$1.07 \times 10^{-4}$	$1.24 \times 10^{-4}$	$1.24 \times 10^{-4}$	$1.23 \times 10^{-4}$
$\dot{Q}_{IDEAL}$ (W)	$1.49 \times 10^4$	$1.10 \times 10^4$	$3.38 \times 10^3$	$5.35 \times 10^4$	$3.62 \times 10^4$	$1.01 \times 10^4$

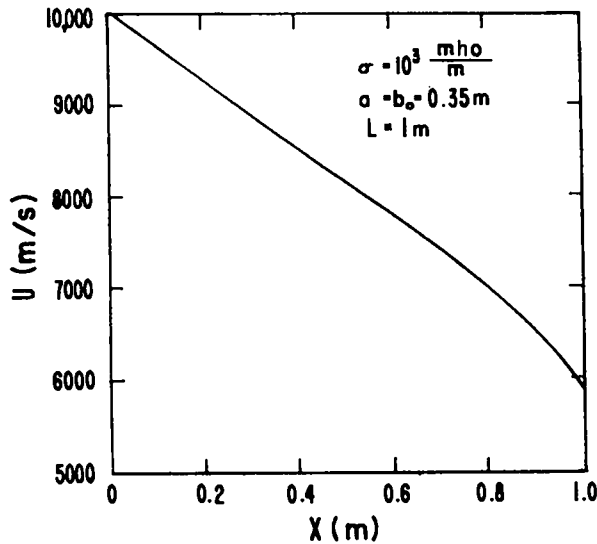


Fig. 7. Velocity distribution in a constant area supersonic channel.

values for comparison purposes that have not been optimized in any way. The reference parameters chosen for the induction coils and for the magnet listed in Table IV were used to determine the results presented in Table V for the three values of plasma conductivity.

It can be seen from Table V that except for the low-conductivity case, the net power of the system,  $\dot{Q}_{\text{net}}$ , is positive for selected reference magnet and induction coil parameters. By changing various magnet and induction coil parameters, it is possible to make  $\dot{Q}_{\text{net}}$  positive also for the low plasma conductivity case. For example, the induction coil current,  $I_{\text{IC}}$ , is below the maximum permissible value,  $I_{\text{MAX}}$ , and, by increasing

TABLE IV

REFERENCE INDUCTION COILS AND MAGNET PARAMETERS

Induction Coil

No. of coils = 2  
 No. of turns (both coils),  $n_{\text{IC}} = 50$   
 No. of turns in 1 layer (both coils),  $m_{\text{IC}} = 10$   
 No. of layers = 5  
 Coil width,  $w_{\text{IC}} = 0.05 \text{ m}$   
 Coil wire diameter,  $d_{\text{IC}} = 0.01 \text{ m}$   
 Current through coils,  $I_{\text{IC}} = 500 \text{ A}$

Magnet

No. of turns in coil,  $n_{\text{MC}} = 6000$   
 No. of turns in 1 layer,  $m_{\text{MC}} = 1000$   
 No. of layers = 6  
 Coil wire diameter,  $d_{\text{MC}} = 0.004 \text{ m}$

TABLE V

EFFECT OF PLASMA CONDUCTIVITY ON DESIGN AND PERFORMANCE OF REFERENCE INDUCTION COILS AND MAGNET IN A CONSTANT AREA SUPERSONIC MHD DECELERATOR

$\sigma$ , mho/m	1000	500	100
$V_{\text{IC}}$ , V	$2.19 \times 10^5$	$1.81 \times 10^4$	9620
$I_{\text{MAX}}$ , A	1967	1619	855
$I_{\text{IC}}$ , A	500	500	500
$R_{\text{IC}}$ , $\Omega$	0.03	0.03	0.03
$I_{\text{MC}}$ , A	7.97	13.1	34.3
$R_{\text{MC}}$ , $\Omega$	22.6	22.6	22.6
$S_{\text{M}}$ , m	4.0	4.0	4.0
$\dot{Q}_{\text{IDEAL}}$ , W	$5.35 \times 10^4$	$3.62 \times 10^4$	$1.01 \times 10^4$
$\dot{Q}_{\text{ICP}}$ , W	$1.36 \times 10^4$	$1.12 \times 10^4$	5911
$\dot{Q}_{\text{IC}}$ , W	9.34	9.30	9.24
$\dot{Q}_{\text{MC}}$ , W	1432	3854	$2.66 \times 10^4$
$\dot{Q}_{\text{net}}$ , W	$1.22 \times 10^4$	7330	$-2.07 \times 10^4$

$I_{\text{IC}}$  to 850 A, the power produced in the induction coil,  $\dot{Q}_{\text{ICP}}$  ( $\dot{Q}_{\text{eL}} \cdot t_{\text{pulse}} \cdot n_{\text{pulse}}$ ) can be increased to  $10^4 \text{ W}$  and the joule loss in the induction coils,  $\dot{Q}_{\text{OICP}}$  ( $\dot{Q}_{\text{OIC}} \cdot t_{\text{pulse}} \cdot n_{\text{pulse}}$ ) will increase to only 21.7 W, still a small value. Using a magnet with 8 layers of 1000 turns instead of 6 layers and a coil wire diameter of 0.006 m instead of 0.004 m will reduce the current in the magnet coil,  $I_{\text{MC}}$ , to 25.7 A and the resistance,  $R_{\text{MC}}$ , to 13.4  $\Omega$ . The joule loss in the magnet coil,  $\dot{Q}_{\text{QMC}}$ , will then be 8847 W. Therefore, a net power of 1131 W will be generated. However, for this design, the magnet arc length,  $S_{\text{M}}$ , will increase from 4 to 6 m, resulting in a larger magnet (2.7- by 2.7- by 1-m with a 2- by 2-m bore rather than the previous 2.03- by 2.03- by 1-m with a 1.33- by 1.33-m bore) and probably in higher cost.

Despite many ways of maximizing  $\dot{Q}_{\text{net}}$ , it can be said that  $\sigma = 100 \text{ mho/m}$  represents the minimum conductivity for which an electromagnet of reasonable size operating in steady state can be designed. Should the conductivity be below 100 mho/m, it will be necessary to either pulse

the magnet or to use superconductors, but the power output will be too low to make this a workable alternative.

From Table V, it can be seen that the reference  $I_{IC}$  is substantially less than  $I_{MAX}$  in cases of  $\sigma=500$  and  $1000$  mho/m; therefore, the net power can be increased by increasing  $I_{IC}$  or by increasing the number of turns in the induction coils so that the voltage across the coils,  $V_{IC}$ , increases. The choice of a suitable operating current and voltage will depend on external load circuit elements and was not considered in this study.

From Table V, it can also be seen that the power dissipated in the induction coil,  $\dot{Q}_{\Omega ICP}$ , is small in comparison to ideal and net generated powers. Increasing  $I_{IC}$  to  $I_{MAX}$  for any  $\sigma$  will not increase the value of  $\dot{Q}_{\Omega ICP}$  significantly compared to the other powers; therefore, this loss has been neglected in the determination of parameters listed in Table IV.

Figure 8 shows the effect of plasma conductivity on the power allocations for a constant area supersonic channel. The joule loss in the induction coils is not shown because it is negligible. It can be seen that the power available from the channel,  $\dot{Q}_{IDEAL}$ , decreases rapidly and the joule loss in the magnet,  $\dot{Q}_{\Omega MC}$  increases rapidly as the conductivity decreases. Comparison of  $\dot{Q}_{IDEAL}$  and  $\dot{Q}_{ICP}$  shows that the power obtained from the induction coils operated at  $I_{IC} = 500$  A approaches the power available at low conductivities. Therefore, the maximum net power,  $\dot{Q}'_{net} = \dot{Q}_{IDEAL} - \dot{Q}_{\Omega MC}$  is generally much higher than  $\dot{Q}_{net} = \dot{Q}_{ICP} - \dot{Q}_{\Omega MC}$ . The operating envelope is between the curves  $\dot{Q}'_{net}$  and  $\dot{Q}_{net}$ . Maximum net powers of  $5 \times 10^4$  W and  $3 \times 10^4$  W can be obtained at conductivities of  $1000$  and  $500$  mho/m respectively. At lower conductivities, but above  $100$  mho/m, the magnet must be redesigned to reduce  $\dot{Q}_{\Omega MC}$ ; otherwise, external power would be required to energize it.

Changing the channel inlet shape does not affect the results greatly. For example, when  $\sigma = 1000$  mho/m, the ideal power changes from  $5.35 \times 10^4$  W for a  $0.35$  by  $0.35$  m channel to  $4.34 \times 10^4$  W for a channel with a width of  $0.25$  m and a

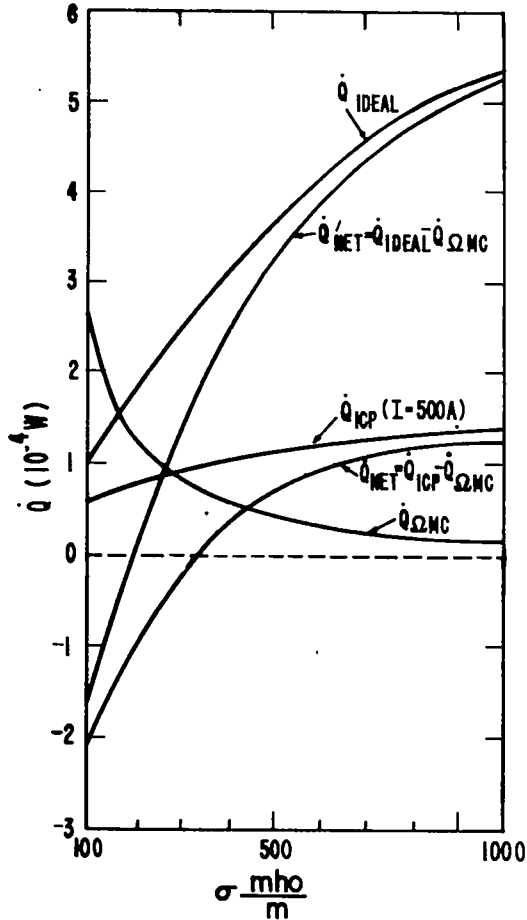


Fig. 8. Effect of conductivity on power allocation for a constant area supersonic channel.

height of  $0.5$  m and to  $6.08 \times 10^4$  W for a channel with a width of  $0.5$  m and a height of  $0.25$  m.

To summarize, a  $0.35$ -m by  $0.35$ - by  $1$ m channel can decelerate the flow from  $10^4$  m/s to approximately  $5800$  m/s (a  $66\%$  decrease in kinetic energy). Maximum power outputs of  $5 \times 10^4$  W and  $3 \times 10^4$  W may be obtained if the plasma conductivity is  $1000$  and  $500$  mho/m, respectively. For conductivities between  $100$  and  $500$  mho/m, the magnet must be designed carefully to minimize the dissipative losses. Below  $100$  mho/m, pulsed or superconducting magnets must be used; this may be economically infeasible because of the low power outputs. A summary description of a typical constant area decelerator is presented in Table VI.

TABLE VI

SUMMARY DESCRIPTION OF A CONSTANT AREA SUPERSONIC DECELERATOR FOR  $\sigma = 1000$  mho/mChannel

Height = 0.35 m  
 Width = 0.35 m  
 Length = 1 m  
 Mass flow rate = 5 kg/s  
 Pulse rate = 10 Hz  
 Inlet velocity =  $10^4$  m/s  
 Exit velocity = 5784 m/s  
 Inlet Mach number = 1.844  
 Exit Mach number = 1.007  
 Inlet pressure =  $10^5$  N/m<sup>2</sup>  
 Exit pressure =  $1.94 \times 10^5$  N/m<sup>2</sup>  
 Ratio of specific heats = 1.2  
 Plasma electric conductivity =  $10^3$  mho/m

Induction Coils

Number of coils = 2  
 Number of turns in both coils = 50  
 Number of turns in 1 layer (both coils) = 10  
 Number of layers = 5  
 Coil width = 0.05 m  
 Coil height = 0.35 m  
 Coil length = 1 m  
 Coil wire diameter = 0.01 m  
 Maximum current allowed = 1967 A  
 Actual current through coils = 500 A  
 Resistance in coils = 0.03  $\Omega$   
 Voltage across coils =  $2.19 \times 10^5$  V

Magnet

Magnetic field = 0.134 T  
 Number of turns in coil = 6000  
 Number of turns per layer = 1000  
 Number of layers = 6  
 Coil wire diameter = 0.004 m  
 Current through coil = 7.97 A  
 Resistance of coil = 22.6  $\Omega$   
 Magnet arc length = 4 m  
 Air gap = 0.45 m  
 Bore in magnet = 1.33 m by 1.33 m  
 Magnet length = 1 m  
 Magnet height = 2.03 m  
 Magnet width = 2.03 m  
 Thickness of magnet = 0.35 m

Power

Ideal power =  $5.35 \times 10^4$  W  
 Total power produced in induction coils  
 =  $1.36 \times 10^4$  W  
 Joule loss in induction coils = 9.34 W  
 Joule loss in magnet coil = 1432 W  
 Net power =  $1.22 \times 10^4$  W

2. Diverging supersonic channel

The inlet conditions and the reference channel and induction coil parameters of the supersonic constant area channel will be retained; however, the geometry of the channel will be changed. For comparison with the constant area

TABLE VII

## EFFECTS OF EXIT HEIGHT ON CHANNEL PARAMETERS OF A DIVERGING SUPERSONIC CHANNEL

Case	1	2	3	4	5
a, m	0.35	0.35	0.35	0.35	0.35
b <sub>o</sub> , m	0.35	0.35	0.35	0.35	0.35
b <sub>f</sub> , m	0.35	0.4	0.5	0.6	0.7
L, m	1	1	1	1	1
B <sub>o</sub> , T	0.134	0.134	0.134	0.134	0.134
$\sigma$ , mho/m	1000	1000	1000	1000	1000
M <sub>o</sub>	1.844	1.844	1.844	1.844	1.844
M <sub>f</sub>	1.007	1.187	1.298	1.335	1.341
U <sub>e</sub> , m/s	5784	6738	7320	7523	7563
P <sub>f</sub> , N/m <sup>2</sup>	$1.94 \times 10^5$	$1.42 \times 10^5$	$1.04 \times 10^5$	$8.40 \times 10^4$	$7.17 \times 10^4$
$\tau$ PULSE, s	$1.24 \times 10^{-4}$	$1.20 \times 10^{-4}$	$1.15 \times 10^{-4}$	$1.12 \times 10^{-4}$	$1.10 \times 10^{-4}$
Q <sub>IDEAL</sub> , W	$5.35 \times 10^4$	$5.91 \times 10^4$	$6.98 \times 10^4$	$8.03 \times 10^4$	$9.05 \times 10^4$

reference case, the inlet cross section will be 0.35m by 0.35m and the length of the channel 1m. The width, a, will be held constant along the length of the channel to avoid a large air gap in the magnet, but the exit height, b<sub>f</sub>, will be varied.

Table VII shows the effects of varying channel height from 0.4 to 0.7m on channel parameters

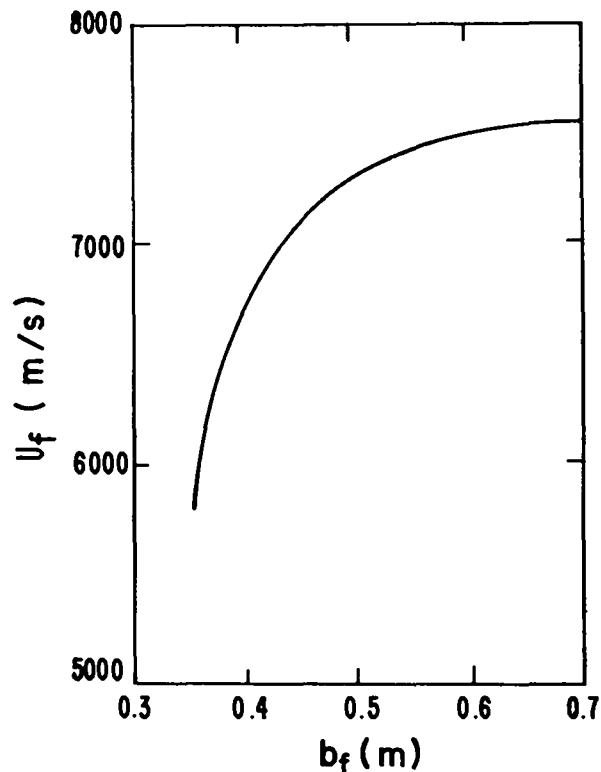


Fig. 9. Exit velocity versus exit height for a diverging supersonic channel.

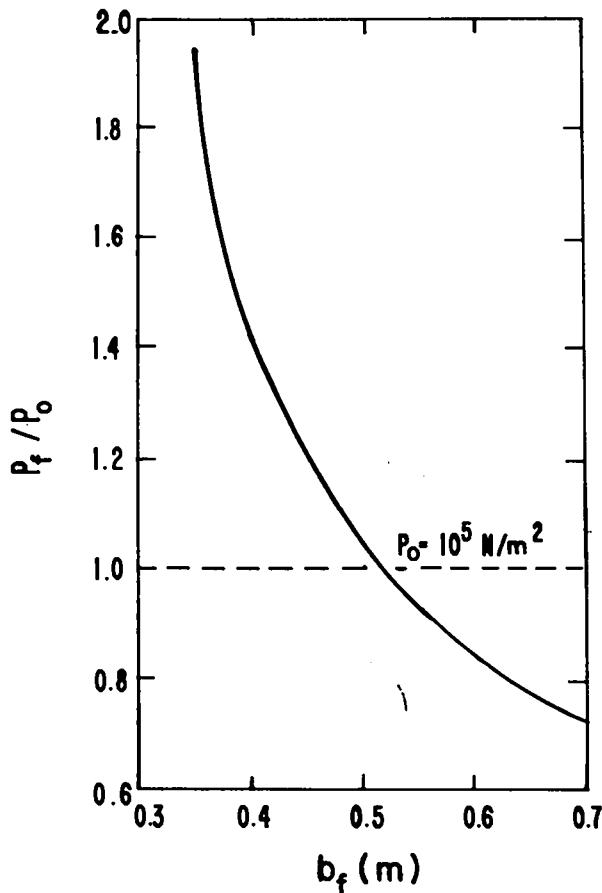


Fig. 10. Exit pressure versus exit height for diverging supersonic channel.

with  $\sigma$  and  $B_0$  held constant. Case 1 is the reference case for the supersonic constant area channel. The maximum channel exit height was limited to 0.7m (corresponding to an expansion angle of  $9.9^\circ$ ) because one-dimensional analysis becomes progressively worse as  $b_f$  increases and the flow, somewhere between 0.7m and 0.9m, changes from decelerating to accelerating.

Figures 9, 10, and 11 show the exit velocity, exit pressure, and ideal power as a function of exit height. As can be seen, the exit velocity increases monotonically and levels off as the exit height increases. This indicates that the velocity gradient is approaching zero and that a further increase in height will accelerate the flow. The exit pressure undergoes transition at  $b_f = 0.52m$ , and for larger  $b_f$  is lower than the inlet pressure  $P_0$ . However, the ideal power continues to increase steadily (linearly) because the volume is increasing.

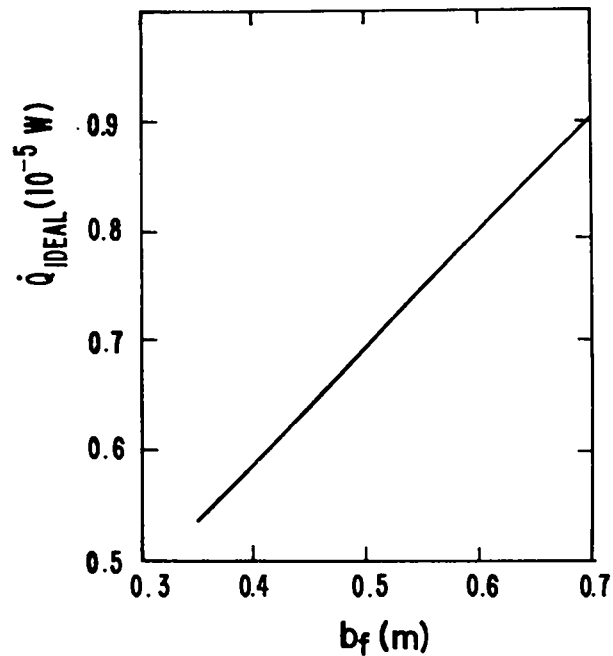


Fig. 11. Ideal power versus exit height for a diverging supersonic channel.

In the following investigation, the channel exit height will be kept at 0.7m and conductivity at 1000 mho/m, while the magnetic field will be varied to obtain nearly sonic conditions at the exit. The parameters resulting in approximately sonic conditions at the exit are the reference case for the supersonic diverging channel and are summarized in Table VIII.

Comparison of Tables VI and VIII shows that the supersonic diverging channel can decelerate the flow to approximately the same velocity as the constant area channel; however, it generates nearly twice as much power. The magnet for the diverging channel is larger because the core must be at least as thick as the channel exit is high. In addition, the induction coils for the diverging channel should be trapezoidal instead of rectangular to minimize joule losses.

Table IX shows the effects of conductivity and size on various parameters using magnet and induction coil characteristics from Table VIII. Column 1 is the reference case for the supersonic diverging channel and Columns 2 and 3 show the effects of varying  $\sigma$ . In each case, the magnetic field was adjusted to obtain near-sonic conditions at the exit. The dependence of the required magnetic field on conductivity is shown in Fig. 12

TABLE VIII

SUMMARY DESCRIPTION OF A DIVERGING SUPERSONIC  
DECELERATOR FOR  $\sigma = 1000$  mho/m

Channel

Inlet height = 0.35 m  
Width = 0.35 m  
Exit height = 0.7 m  
Length = 1 m  
Mass flow rate = 5 kg/s  
Pulse rate = 10 Hz  
Inlet velocity =  $10^4$  m/s  
Exit velocity = 5815 m/s  
Inlet Mach number = 1.844  
Exit Mach number = 1.005  
Inlet pressure =  $10^5$  N/m<sup>2</sup>  
Exit pressure =  $9.82 \times 10^4$  N/m<sup>2</sup>  
Ratio of specific heats = 1.2  
Plasma electric conductivity =  $10^3$  mho/m

Induction coils

Number of coils = 2  
Number of turns (both coils) = 50  
Number of turns in 1 layer (both coils) = 10  
Number of layers = 5  
Coil width = 0.05 m  
Coil height at duct inlet = 0.35 m  
Coil height at duct exit = 0.7 m  
Coil length = 1 m  
Coil wire diameter = 0.01 m  
Maximum current allowed = 2318 A  
Actual current through coils = 500 A  
Resistance in coils = 0.03  $\Omega$   
Voltage across coils =  $3.83 \times 10^4$  V

Magnet

Magnetic field = 0.157 T  
Number of turns in coil = 6000  
Number of turns in 1 layer = 1000  
Number of layers = 6  
Coil wire diameter = 0.004 m  
Current through coil = 9.37 A  
Resistance of coil = 76.6  $\Omega$   
Magnet arc length = 4 m  
Air gap = 0.45 m  
Bore in magnet = 1.33 m by 1.33 m  
Magnet length = 1 m  
Magnet height = 2.73 m  
Magnet width = 2.73 m  
Thickness of magnet = 0.7 m

Power

Ideal power =  $1.08 \times 10^5$  W  
Total power produced in induction coils =  $2.33 \times 10^4$  W  
Joule loss in induction coils = 10.4 W  
Joule loss in magnet coil = 2494 W  
Net power from system =  $2.07 \times 10^4$  W

and the power allocations as a function of  $\sigma$  are shown in Fig. 13.

In comparison with the constant area supersonic channel, the diverging channel has twice as much available power ( $10^5$  W for  $\sigma = 1000$  mho/m) for nearly the same exit velocity. The increase

TABLE IX

EFFECTS OF CONDUCTIVITY AND SIZE ON PARAMETERS OF A  
DIVERGING AREA SUPERSONIC CHANNEL

	$\sigma$ , mho/m			
	1000	500	100	$L=1.5, b_f=1.05$
$a_0$ , m	0.35	0.35	0.35	0.35
$b_0$ , m	0.35	0.35	0.35	0.35
$b_f$ , m	0.7	0.7	0.7	1.05
$L$ , m	1.0	1.0	1.0	1.5
$B_0$ , T	0.157	0.256	0.670	0.120
$\sigma$ , mho/m	1000	500	100	1000
$M_0$	1.844	1.844	1.844	1.844
$M_f$	1.005	1.011	1.009	1.026
$U_f$ , m/s	5815	5872	5904	5940
$P_f$ , N/m <sup>2</sup>	$9.82 \times 10^4$	$9.80 \times 10^4$	$9.89 \times 10^4$	$6.72 \times 10^4$
$\tau_{PULSE}$ , s	$1.21 \times 10^{-4}$	$1.20 \times 10^{-4}$	$1.19 \times 10^{-4}$	$1.74 \times 10^{-4}$
$Q_{IDEAL}$ , W	$1.08 \times 10^5$	$7.27 \times 10^4$	$2.05 \times 10^4$	$2.04 \times 10^5$
$V_{IC}$ , V	$3.83 \times 10^4$	$3.18 \times 10^4$	$1.71 \times 10^4$	$4.2 \times 10^4$
$I_{MAX}$ , A	2317	1905	1008	2781
$I_{IC}$ , A	500	500	500	500
$\dot{Q}_{ICP}$ , W	$2.33 \times 10^4$	$1.91 \times 10^4$	$1.02 \times 10^4$	$3.65 \times 10^4$
$\dot{Q}_{QICP}$ , W	10.4	10.3	10.2	21.8
$\dot{Q}_{QMC}$ , W	2494	6632	$4.54 \times 10^4$	2222
$\dot{Q}_{NET}$ , W	$2.07 \times 10^4$	$1.25 \times 10^4$	$-3.53 \times 10^4$	$6.72 \times 10^4$

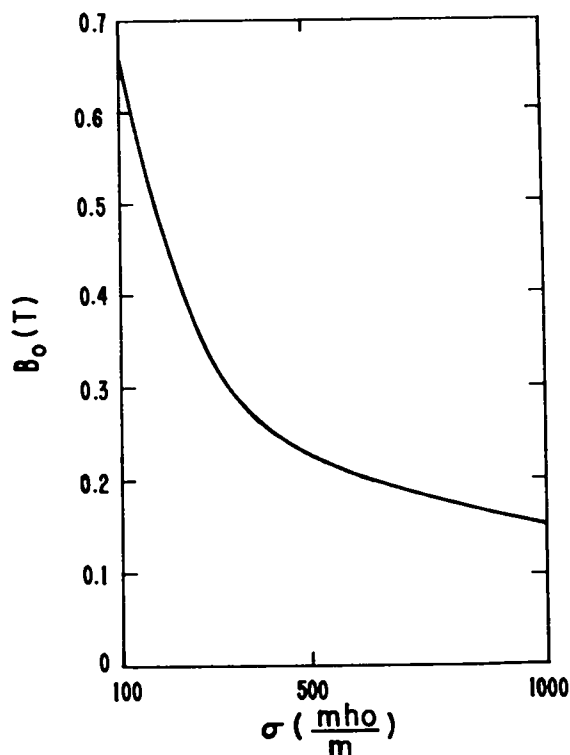


Fig. 12. Magnetic field required to attain near-sonic conditions at the exit of a diverging supersonic channel.



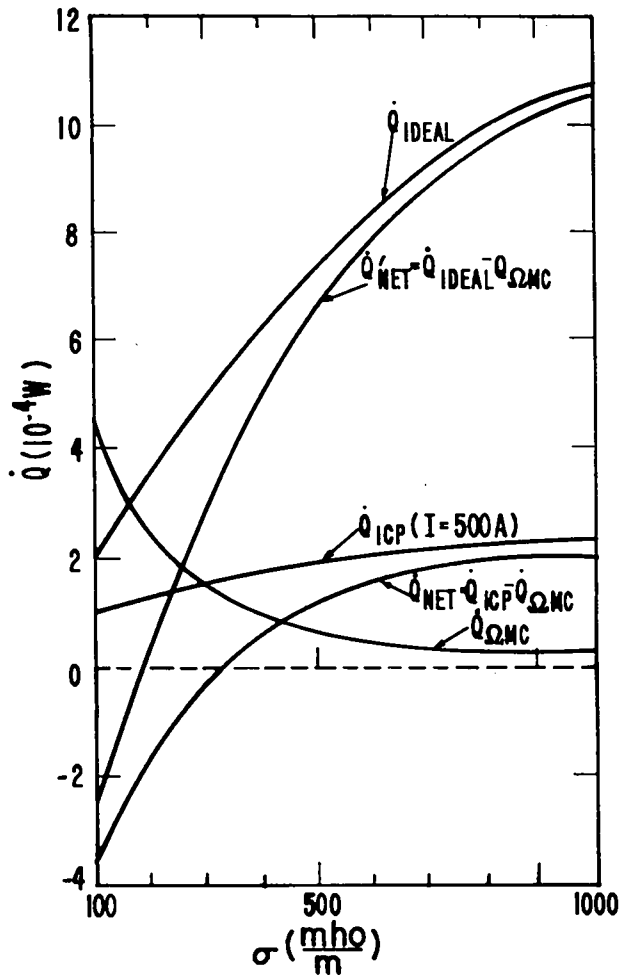


Fig. 13. Effect of conductivity on power allocation for a diverging supersonic channel.

in power is accompanied by a modest increase in the magnet size from 2m by 2m to 2.7m by 2.7m.

The last column in Table IX shows the effect of increasing the length of the channel to 1.5m, and the exit height to 1.05m; the magnetic field was decreased, as required, to keep the Mach number at the exit near unity. As a result of these changes, the power nearly doubled, but the magnet dimensions increased from 2.7m by 2.7m by 1m to 3.4 by 3.4 by 1.5m. Therefore, more power can be obtained for the price of a physically larger system and a cost trade-off must be carried out to determine the optimum size and performance.

Finally, note that without electromagnetic forces, a supersonic flow can be slowed down only in a converging channel ( $dA/dx < 0$ ). Since, in supersonic flow, the electromagnetic terms in Eq. (13) have negative signs, a converging channel

with electromagnetic forces would be more effective in decelerating flow than an ordinary supersonic diffuser. However, it may lead to shocks and therefore require a more extensive analysis than was intended in the present preliminary study.

### 3. Subsonic flow decelerator

Equation (13) shows that when the flow is subsonic, it is decelerated by the geometric term,  $dA/dx$ , but is accelerated by the electromagnetic terms. Therefore, a subsonic diffuser will decelerate the flow more efficiently than any subsonic MHD decelerator. Consequently, the question to be asked is: can a subsonic MHD-decelerator be designed to produce sufficient power and be sufficiently small to compete with the diffuser?

For plasma inlet conditions fixed in this study, an inlet area exceeding  $0.42m^2$  is required for subsonic flow. Therefore, an inlet 0.7m wide and 0.7m high was assumed for the investigation. In addition, the exit height of 1.0m and the length of 1.5m were chosen.

In supersonic flow, the magnetic field is limited by the constraint that the flow inside the channel not become subsonic, while in subsonic flow the magnetic field is limited by the fact that too large a field will accelerate the flow. The latter occurs when the electromagnetic terms exceed the geometric term in the momentum conservation equation.

The effect of a magnetic field on the performance characteristics of a subsonic MHD decelerator is shown in Table X for  $\sigma=1000$  mho/m. Note that the magnetic field strength is limited to very small values, i.e., to  $\sim 0.04$  T or less. Also, it can be seen that as the magnetic field increases, the exit velocity increases; this is consistent with the previous statement that a diffuser is better than an MHD decelerator in decelerating subsonic flows. By comparing Column 1 of Table X with Column 4 of Table III and with Column 1 of Table IX, it is seen that the supersonic decelerators slow down the flow to nearly the same exit velocity as the subsonic decelerators, and, in addition, provide more power in a smaller volume (higher power densities) because of their larger magnetic fields. In the case of the subsonic decelerator, the flow may be slowed down further by decreasing the magnetic field, but the

TABLE X

EFFECT OF MAGNETIC FIELD ON PERFORMANCE CHARACTERISTICS OF A DIVERGING SUBSONIC CHANNEL<sup>a</sup>

$B_0$ , T	0.02	0.03	0.04
$\sigma$ , mho/m	$10^3$	$10^3$	$10^3$
$M_0$	0.922	0.922	0.922
$M_f$	0.507	0.533	0.588
$U_f$ , m/s	5796	6070	6628
$P_f$ , N/m <sup>2</sup>	$1.35 \times 10^5$	$1.28 \times 10^5$	$1.15 \times 10^5$
$t_{PULSE}$ , s	$2.11 \times 10^{-4}$	$2.04 \times 10^{-4}$	$1.92 \times 10^{-4}$
$\dot{Q}_{IDEAL}$ , W	$1.98 \times 10^4$	$4.69 \times 10^4$	$9.19 \times 10^4$

<sup>a</sup>Channel inlet: 0.7 by 0.7 m,  
Channel exit: 0.7 by 1.0 m,  
Channel length: 1.5 m.

corresponding power will also decrease. This result confirms that a diffuser is the best decelerator of subsonic flows.

Increasing the generator exit height to 2.8 m, the length to 3.0 m, and the magnetic field to 0.07 T will decelerate the flow to 2872 m/s and will result in an available power of  $7.69 \times 10^5$  W. However, a 6.93-m by 6.93-m by 3.0-m magnet would be required to attain such power extraction. The large generator size is a consequence of the fact that for a given inlet area, length, and magnetic field, an exit height exists below which the flow will accelerate and only above which it will decelerate.

A summary description of the subsonic decelerator is presented in Table XI.

#### 4. MHD Decelerator with Electrodes

Because the lifetime of electrodes poses a sufficiently serious problem to cast doubt on the feasibility of their use in MHD decelerators, it will not be discussed in any detail. We compared the reference cases for the induction decelerators listed in Tables VI, VIII, and XI with corresponding decelerators with electrodes. All pertinent parameters listed in Tables VI, VIII, and XI were used to determine the characteristics of the decelerators with electrodes. The load parameter,  $K$ , was taken to be 1/2, to maximize the power density.

TABLE XI

SUMMARY DESCRIPTION OF A DIVERGING SUBSONIC DECELERATOR WITH  $\sigma = 1000$  mho/m

#### Channel

Inlet height = 0.7 m  
Width = 0.7 m  
Exit height = 2.8 m  
Length = 3.0 m  
Mass flow rate = 5 kg/s  
Pulse rate = 10 Hz  
Inlet velocity =  $10^4$  m/s  
Exit velocity = 2872 m/s  
Inlet Mach number = 0.922  
Exit Mach number = 0.235  
Inlet pressure =  $10^5$  N/m<sup>2</sup>  
Exit pressure =  $1.10 \times 10^5$  N/m<sup>2</sup>  
Ratio of specific heats = 1.2  
Plasma electric conductivity =  $10^3$  mho/m

#### Induction Coil

Number of coils = 2  
Number of turns (both coils) = 50  
Number of turns in 1 layer (both coils) = 10  
Number of layers = 5  
Coil width = 0.05 m  
Coil height at duct inlet = 0.7 m  
Coil height at duct exit = 2.8 m  
Coil length = 3.0 m  
Coil wire diameter = 0.01 m  
Maximum current allowed = 3571 A  
Actual current through coils = 500 A  
Resistance in coils = 0.11  $\Omega$   
Voltage across coil =  $2.96 \times 10^4$  V

#### Magnet

Magnetic fields = 0.07 T  
Number of turns in coil = 6000  
Number of turns in 1 layer = 1000  
Number of layers = 6  
Coil wire diameter = 0.004 m  
Current through coil = 7.43 A  
Resistance of coil = 96.9  $\Omega$   
Magnet arc length = 4 m  
Air gap = 0.8 m  
Bore in magnet = 1.33 m by 1.33 m  
Magnet length = 3.0 m  
Magnet height = 6.93 m  
Magnet width = 6.93 m  
Thickness of magnet = 2.8 m

#### Power

Ideal power =  $7.69 \times 10^5$  W  
Total power produced in induction coils =  $1.08 \times 10^9$  W  
Joule loss in induction coils = 200 W  
Joule loss in magnet coil = 5350 W  
Net power from system =  $1.02 \times 10^5$  W

We found it necessary to shorten the supersonic electrode-type decelerator to 0.93m, to maintain a slightly supersonic flow at the exit.

Exit velocities and ideal powers for the induction- and electrode-type decelerators are compared in Table XII. It can be seen that the performances are nearly equal. In general, the induction-type decelerator generates slightly more power because the average magnetic Reynold's number along the channel is slightly greater than unity.

#### V. CONCLUDING OBSERVATIONS

The following conclusions may be inferred from the investigation reported here.

- The inlet area is a critical parameter of the MHD decelerator because it determines the inlet Mach number and, therefore, the flow regime. For the inlet conditions given in this report, supersonic flow occurs for inlet areas less than  $0.42\text{m}^2$  and subsonic flow occurs for inlet areas greater than  $0.42\text{m}^2$ .
- For supersonic inlet conditions the restriction to shockless flow limits the magnetic field and, for a given plasma conductivity, the power output of the device. A small inlet area (0.35m by 0.35m) was required to obtain a sufficiently high inlet Mach number, so that a reasonably strong magnetic field could be used to obtain useful power output and to decelerate the flow sufficiently. For geometries considered (constant area and diverging channels), the exit Mach number constraint limits the exit velocity to 5800-5900 m/s. The MHD decelerators are characterized by low magnetic fields, e.g., 0.15 T, and low power output, i.e., less than  $10^5$  W even for  $\sigma=1000$  mho/m.
- A supersonic constant area channel is simpler to construct than a diverging channel and is, also more compact. For example, a 2.0- by 2.0- by 1.0m magnet is required for the constant area reference case while a 2.7- by 2.7- by 1.0m magnet is required for the diverging decelerator. However, the latter will produce more power because of its larger volume.
- For either supersonic or subsonic channels, net power production with steady-state magnet operation is possible only when the conductivity is higher than 100mho/m. For lower plasma conductivities, pulsed or superconducting magnets must be used; however, the low power outputs at such low conductivities indicate that this solution may be economically infeasible. Consequently, the induction decelerators should operate with plasma conductivities of 100mho/m or higher if they are to be considered for slowing down fuel pellet debris ions and for extracting energy in the process. For low conductivities, the magnet should be designed with care to prevent joule losses in coils from becoming so high that external power may be required to operate the device.

TABLE XII  
COMPARISON OF INDUCTION AND ELECTRODE-TYPE DECELERATORS

	Induction Type		Electrode Type*	
	$U_f$ , m/s	$\dot{Q}_{IDEAL}$ , W	$U_f$ , m/s	$\dot{Q}_{IDEAL}$ , W
Supersonic constant area	5784	$5.35 \times 10^4$	5840	$4.62 \times 10^4$
Supersonic diverging area	5815	$1.08 \times 10^5$	5281	$9.21 \times 10^4$
Subsonic diverging area	2872	$7.69 \times 10^5$	2655	$5.23 \times 10^5$

\*Length of decelerator shortened to 0.93 m to meet the constraint of exit Mach number = 1.

- For subsonic decelerators, the magnetic field is constrained by the restriction to decelerating flows and cannot exceed the critical value at which the flow will change to an accelerating one. Conversely, for a given field, channel length, and inlet area, increasing the exit height past a critical value will change the flow from accelerating to decelerating one. Therefore, subsonic decelerators are always larger than supersonic.
- Subsonic decelerators are most efficient when no electromagnetic forces are acting on the plasma, i.e., subsonic diffusers. A MHD decelerator will be competitive with the diffuser only if sufficient power is produced in a device of reasonable size and at an acceptable exit velocity.
- Because of the factors mentioned above, the subsonic decelerators will have very small fields, e.g., less than 0.1 T for a conductivity of 1000 mho/m. Even for this high conductivity, the channels will be large. For example, a 7- by 7- by 3-m magnet would be required to produce  $10^5$  W or more and to reduce the exit velocity to 2900 m/s.
- Increasing the size of either subsonic or supersonic channels will increase the power, but will also increase costs; the amount of increase was not investigated in this study.
- The performances of induction and electrode-type decelerators are approximately equal. The induction-type decelerator generates slightly more power because the average magnetic Reynolds number along the channel is slightly greater than unity for the conditions studied in this report. However, the electrode-type decelerator may not be feasible because of limited electrode lifetime in the plasma environment anticipated for inertial confinement fusion reactors.

The preliminary conclusions derived from the analysis presented in this report indicate that induction-type MHD decelerators merit serious consideration for processing reaction products in inertial confinement fusion reactors and for energy extraction.

#### ACKNOWLEDGMENTS

The authors thank Patricia Rood for assistance in coding and performing the calculations reported here.

#### REFERENCES

1. T. Frank, D. Freiwald, T. Merson, and J. Devaney, "A Laser Fusion Reactor Concept Utilizing Magnetic Fields for Cavity Wall Protection," Proc. ANS 1st Topical Meeting on the Tech. of Controlled Nuclear Fusion, San Diego, CA (1974), V. I, p. 83.
2. I. O. Bohachevsky and J. F. Hafer, "Sputtering Erosion of Fusion Reactor Cavity Walls," Los Alamos Scientific Laboratory report LA-6633-MS (December 1976).
3. I. O. Bohachevsky, "MHD Deceleration in Magnetically Protected Reactor Concept," in "Laser Fusion Program Progress Report, January 1-June 30, 1977," Los Alamos Scientific Laboratory report LA-6982-PR (April 1978), p. 135.
4. P. Britton, "MHD Generators - More Kilowatts from a Ton of Coal," Popular Science 79 (August 1978).
5. S. A. Colgate and R. L. Aamodt, "Plasma Reactor Promises Direct Electric Power," Nucleonics 50-55 (August 1957).
6. E. P. Velikhov, V. S. Goloubev, and V. V. Chermovkha, "On a Possibility of MHD-Conversion of Fusion Reactor Energy," Proc. IAEA Workshop on Fusion Reactor Design Problems, Culham Laboratory, Abingdon, England (1974).
7. A. S. Roberts, Jr., "On the Concept of Pulsed Thermonuclear MHD Energy Conversion," Aktiebolaget Atomenergi, Stockholm, Sweden TPM-FA-869 (1969).
8. A. S. Roberts, Jr., "Proposed Plasma Burst MHD Generator Experiment," Aktiebolaget Atomenergi, Stockholm, Sweden AE-FA-867 (1969).
9. L. Wood and T. Weaver, "Some Direct Conversion Possibilities for Advanced CTR Systems," Lawrence Livermore Laboratory COT/Phys 73-B (1973).
10. T. Weaver, G. Zimmerman, and L. Wood, "Prospects for Exotic Fuel Usage in CTR Systems," Lawrence Livermore Laboratory report UCRL-7191 (1972).
11. G. Lee, G. Zimmerman, and L. Wood, "Concerning Electron-Ion Coupling and Charged Particle Energy Deposition During Vigorous Thermonuclear Burn," Lawrence Livermore Laboratory report UCRL-74192 (1972).
12. G. W. Sutton and A. Sherman, Engineering Magnetohydrodynamics (McGraw-Hill Inc, 1965), 343.

13. R. B. Clark, D. T. Swift-Hook, and J. K. Wright, "The Prospects for Alternating Current Magnetohydrodynamic Power Generation," Brit. J. Appl. Phys. 14, 10-15 (1963).

14. J. C. Goldstein, I. O. Bohachevsky, and D. O. Dickman, "Ion Motion in Laser Fusion Reactor Studies," Paper 9P7, Bull. Am. Phys. Soc. Series 11, 21 (October 1976).

Printed in the United States of America. Available from  
National Technical Information Service  
U.S. Department of Commerce  
5285 Port Royal Road  
Springfield, VA 22161

Microfiche \$3.00

001-025	4.00	126-150	7.25	251-275	10.75	376-400	13.00	501-525	15.25
026-050	4.50	151-175	8.00	276-300	11.00	401-425	13.25	526-550	15.50
051-075	5.25	176-200	9.00	301-325	11.75	426-450	14.00	551-575	16.25
076-100	6.00	201-225	9.25	326-350	12.00	451-475	14.50	576-600	16.50
101-125	6.50	226-250	9.50	351-375	12.50	476-500	15.00	601-up	

Note: Add 52.50 for each additional 100-page increment from 601 pages up.